Journal of Fluorine Chemistry 218 (2019) 42–50

Contents lists available at ScienceDirect

Journal of Fluorine Chemistry

journal homepage: www.elsevier.com/locate/fluor

Semi-fluorinated *p*-terphenyl liquid crystals

Moisés Alberto Valdés-Pech, Leticia Larios-López, Rosa Julia Rodríguez-González, Isaura Felix-Serrano, Nayely Trejo-Carbajal, Dámaso Navarro-Rodríguez*

Departamento de Materiales Avanzados, Centro de Investigación en Química Aplicada, Blvd. Enrique Reyna 140, C.P. 25294, Saltillo, Coahuila, Mexico

ARTICLE INFO

Keywords:
Fluorine
p-terphenyl
Liquid crystal
Fluorescence

ABSTRACT

p-Terphenyls carrying two or four fluorine atoms in the central ring were synthesized via Suzuki-Miyaura cross-coupling reaction using phenylboronic acids and fluorinated dibromobenzenes. By calorimetric and X-ray diffraction analyses it was found that the *p*-terphenyls carrying two fluorine atoms develop nematic and/or smectic (A and C) phases. On the contrary, the *p*-terphenyls substituted with four fluorine atoms are not liquid crystals. Differences found in the thermal behavior are explained in terms $\pi - \pi_F$ interactions arising from the electron withdrawing ability of the fluorine atom. Such $\pi - \pi_F$ interactions let the *p*-terphenyls stack in a staggered configuration that explains the stability of the smectic C phase. On the other hand, the semi-fluorinated *p*-terphenyls absorb and emit in the blue region of the electromagnetic spectrum; a measured large Stokes shift indicates that these compounds are nearly transparent to their own emitted light. This optical characteristic, combined with liquid crystals properties of low order, makes these new *p*-terphenyls potential candidates for linearly polarized blue-emitting layers in electroluminescent devices.

1. Introduction

p-Terphenyls substituted with long terminal chains and short lateral groups (methyl, methoxy, cyano, halogen, etc.) are able to develop liquid crystal phases of low order like nematic and smectic-A phases [1,2]. Under appropriate illumination they are also able to fluoresce in the blue region of the electromagnetic spectrum [3]. In addition, p-terphenyls have excellent thermal stability [4], high dielectric anisotropy [5,6], and high capacity to induce birefringence [7]. These and other properties have been modified (or improved) by exchanging some of their hydrogens for other atoms or short chemical groups. Fluorine, the most electronegative element, has undoubtedly been the most explored substituent in p-terphenyls [8,9]. It turns out that fluorine and hydrogen atoms are similar in size (1.47 and 1.2 Å, respectively), and therefore, the one can replace the other without causing major changes in conformation, although, the electron density distribution and the intermolecular interactions can be altered, leading to different stacking and properties [2,10]. It has been generally found that a partial exchange of hydrogens by fluorine atoms in p-terphenyl liquid crystals shifts the mesomorphic behavior towards lower temperatures, induces the formation of low-ordered (low viscous) mesophases such as the nematic and smectic C phases, enlarges the temperature interval of mesophases, induces negative dielectric anisotropies and chirality, etc. [11–14] p-Terphenyl liquid crystals substituted with cyano groups have also been the subject of numerous reports, particularly those carrying this group at one of its two ends [15,16]. Such cyano-substituted p-terphenyls possess a strong polarization moment due to the high electron withdrawing character of the cyano group. Furthermore, p-terphenyls carrying cyano groups show fairly good thermal, chemical, and photochemical stabilities [17]. p-Terphenyls carrying both fluorine and cyano groups have already been explored [2,16,18], but in only few of them both groups are in lateral positions. Herein, we report on the liquid-crystalline and optical properties of didodecyloxy-p-terphenyls laterally substituted with fluorine and cyano groups.

2. Experimental

2.1. Materials

All reagents were purchased from Aldrich and used without further purification unless otherwise noted. Reactive grade acetone, methanol, chloroform ($CHCl_3$), and hexanes were purchased from J. T. Baker and were used without further purification. Tetrahydrofuran (THF) was dried over a sodium/ benzophenone complex and distilled right before use.

* Corresponding author.
E-mail addresses: moises.valdes.psg@ciqa.edu.mx (M.A. Valdés-Pech), leticia.larios@ciqa.edu.mx (L. Larios-López), julia.rodriguez@ciqa.edu.mx (R.J. Rodríguez-González), isaura.felix.pd@ciqa.edu.mx (I. Felix-Serrano), nayely.trejo.pd@ciqa.edu.mx (N. Trejo-Carbajal), damaso.navarro@ciqa.edu.mx (D. Navarro-Rodríguez).

https://doi.org/10.1016/j.jfluchem.2018.11.011
Received 7 August 2018; Received in revised form 16 November 2018; Accepted 22 November 2018
Available online 29 November 2018

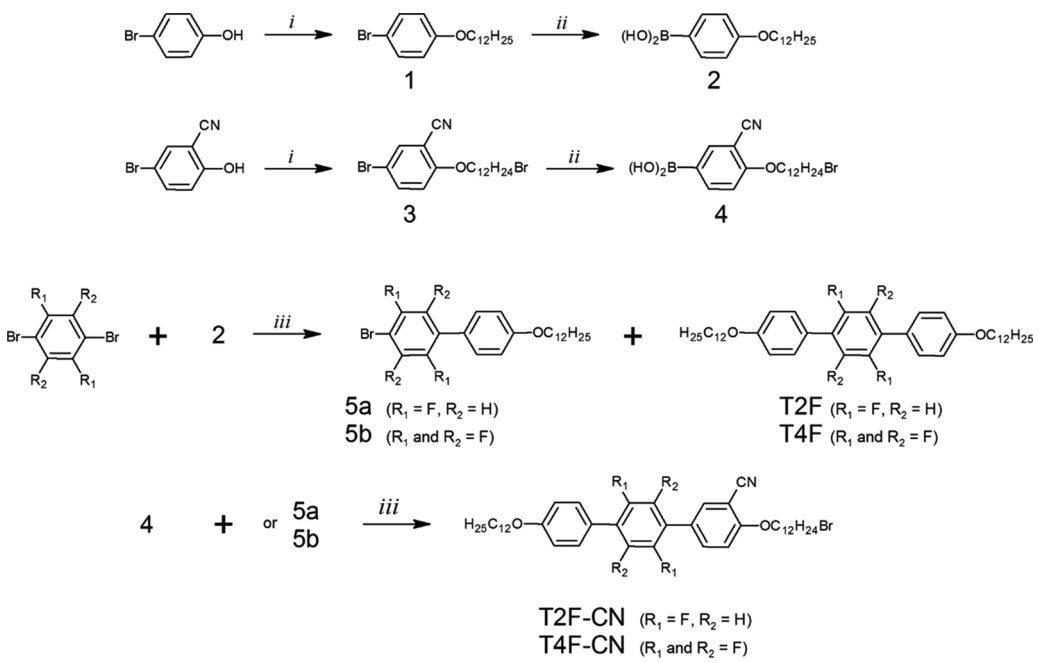

Scheme 1. Route for the synthesis of the semi-fluorinated *p*-terphenyls. *i*) Acetone, K_2CO_3, KI and $C_{12}H_{25}Br$ (or $C_{12}H_{24}Br_2$), 65 °C, 48 h, *ii*) THF, n-BuLi and triisopropyl borate, −40 °C / HCl 2 N, 25 °C, and *iii*) THF, Na_2CO_3 2 M and $Pd[P(C_6H_5)_3]_4$, 65 °C.

2.2. Synthesis

Four partially fluorinated *p*-terphenyls were synthesized according to the route outlined in Scheme 1. Two of them carry two or four fluorine atoms in the central ring and one dodecyloxy chain at each one of the two peripheral rings. These *p*-terphenyls were named T2F and T4F, respectively. The other two *p*-terphenyls are similar to T2F and T4F but they carry one extra cyano group in one peripheral ring, and were named T2F-CN and T4F-CN, respectively. These two later molecules are end-functionalized with one bromine atom because they will be used in further reactions aiming to obtain methacrylate monomers and their corresponding side-chain liquid crystal polymers. Intermediates 1-4 were synthesized according to reported procedures. [3,19] Precursors 5a and 5b, as well as the four semi-fluorinated *p*-terphenyls, were synthesized as described below.

2.2.1. 4-bromo-2,5-difluoro-4'-dodecyloxybiphenyl (5a)

In a 250 mL three-neck round-bottom flask, under magnetic stirring and argon atmosphere, 200 mL of THF (freshly distilled), 4.44 g (16.3 mmol) of 1,4-dibromo-2,5-difluorobenzene, and 0.226 g (0.2 mmol) of $Pd[P(C_6H_5)_3]_4$, were introduced. This mixture was heated to 65 °C before adding 42.5 mL of an aqueous solution of Na_2CO_3 2 M. The reaction was held under stirring for 30 min and then 2 g (6.53 mmol) of 4-dodecyloxyphenyl boronic acid (dissolved in THF) were added dropwise. 72 h later the reaction was stopped and the solvent was evaporated. Then, 200 mL of chloroform were added and the solution was washed three times with water. The chloroform was evaporated and the remaining solid was dried before being re-dissolved in hot chloroform. On cooling this solution, a white solid was precipitated (T2F, yield 28%) and recuperated by filtration. The liquid phase was evaporated and the recuperated solid was recrystallized from hot methanol and filtered. 5a was obtained as a white powder (yield 40%).

5a: ^{1}H NMR ($CDCl_3$, δ = ppm) 0.88 (t, CH_3, 3H, J = 6.6 Hz), 1.19–1.65 (m, CH_2, 18 H), 1.8 (m, O–CH_2–CH_2, 2 H), 4.0 (t, O–CH_2–CH_2, 2H J = 6.6 Hz), 6.95 (d, Ar, 2H, J = 8.5 Hz), 7.18 (dd, Ar, 1H, J = 8.9, 6.7 Hz), 7.34 (dd, Ar, 1H, J = 9.5, 5.9 Hz), 7.45 (d, Ar, 2H, J = 8.5 Hz).

T2F: ^{1}H NMR ($CDCl_3$, δ = ppm) 0.89 (t, CH_3, 6H, J = 6.6 Hz), 1.23–1.54 (m, CH_2, 36 H), 1.8 (m, O–CH_2–CH_2, 4 H), 4.0 (t, O–CH_2–CH_2, 4H, J = 6.6 Hz), 6.98 (d, Ar, 4H, J = 8.8 Hz), 7.19 (t, Ar, 2H, J = 8.9 Hz), 7.51 (d, Ar, 4H, J = 8.5 Hz). FT-IR (KBr, cm^{-1}) 2922 and 2853 (ν CH_2); 1610, 1528, and 1491 (ν C = C ring);1258 (ν C–F); 1187 (ν C–O–C); 1032 (ν C–O); 888, 838 and 792 (δ C–H). FABHRMS: Observed (*m/z*) [M^+] 634.4547 (100%); Estimated [M^+] (*m/z*) 634.4561. *Anal* Calcd for $C_{42}H_{60}F_2O_2$: C, 79.45; H, 9.53; F, 5.98; O, 5.04. Found: C, 79.98; H, 9.76.

2.2.2. 4-bromo-2,3,5,6-tetrafluoro-4'-dodecyloxybiphenyl (5b)

A procedure similar to that used for the synthesis of compound 5a was followed. 5.03 g (16.3 mmol) of 1,4-dibromotetrafluoro benzene, 0.3774 g (0.33 mmol) of $Pd[P(C_6H_5)_3]_4$, 42.5 mL of an aqueous Na_2CO_3 2 M solution, and 2 g (6.53 mmol) of 4-dodecyloxyphenylboronic acid. Two products were obtained as white crystals: T4F (yield 22.8%) and 5b (yield 40%).

5b: ^{1}H NMR ($CDCl_3$, δ = ppm) 0.88 (t, CH_3, 3H, J = 6.9 Hz), 1.22–1.52 (m, CH_2, 18 H), 1.8 (m, O–CH_2–CH_2, 2 H), 4.02 (t, O–CH_2–CH_2, 2H, J = 6.5 Hz), 7.0 (d, Ar, 2H, J = 8.8 Hz), 7.38 (d, Ar, 2H, J = 8.8 Hz).

T4F: ^{1}H NMR ($CDCl_3$, δ = ppm) 0.89 (t, CH_3, 6H, J = 6.5 Hz), 1.19–1.55 (m, CH_2, 36 H), 1.80 (m, O–CH_2–CH_2, 4 H), 4.02 (t, O–CH_2–CH_2, 4H, J = 6.6 Hz), 7.01 (d, Ar, 4H, J = 8.8 Hz), 7.42 (d, Ar, 4H, J = 8.5 Hz). FT-IR (KBr, cm^{-1}): 2923 and 2854 (ν CH_2); 1613, 1530, and 1469 (ν C = C ring); 1250 (ν C–F); 1176 (ν C–O–C); 1028 (ν C–O); 822 and 725 (δ C–H).

2.2.3. 4-(ω-bromododecyloxy)-2′,5′-difluoro-4″-dodecyloxy-1,1′:4′,1″-terphenyl-3-carbonitrile (T2F-CN)

In a 250 mL three-neck round-bottom flask, under stirring and argon atmosphere, 200 mL of THF (freshly distilled), 1.137 g (2.51 mmol) of 5a, and 0.145 g (0.125 mmol) of $Pd[P(C_6H_5)_3]_4$, were introduced. This mixture was heated to 70 °C before adding 16.3 mL of Na_2CO_3 2 M (aqueous solution), and 1.2342 g (3.01 mmol) of 3-cyano-4-(ω-bromododecyloxy) phenylboronic acid. The reaction was held at 70 °C and stirring for 72 h. Once this time has elapsed, the solution was allowed to cool down to room temperature and 100 mL of ethyl ether were added. The solution was filtered and the solid was transferred to a separation funnel where it was washed three times with distilled water. The ether

phase was evaporated and the solid was suspended in $CHCl_3$. Finally, the product was purified by column chromatography (silica gel) using a hexanes:ethyl acetate (95:5) mixture as eluent. T2F-CN was obtained as a white solid (yield 66.7%). ^{1}H NMR ($CDCl_3$, δ = ppm) 0.86 (t, CH_3, 3H, J = 6.6 Hz), 1.2–1.6 (m, CH_2, 34 H), 1.7–1.9 (m, O–CH_2–CH_2, Br–CH_2–CH_2, 6 H), 3.41 (t, CH_2–Br, 2H, J = 6.9 Hz), 4.0 (t, O-CH_2–CH_2, 2H, J = 6.6 Hz), 4.12 (t, O-CH_2–CH_2, 2H, J = 6.5 Hz), 6.98 (d, Ar, 2H, J = 9.1 Hz), 7.05 (d, Ar, 1H, J = 9.1 Hz), 7.15 (dd, Ar, 1H, J = 10.7, 6.6 Hz), 7.22 (dd, Ar, 1H, J = 11.0, 6.6 Hz), 7.5 (dd, Ar, 2H, J = 8.8, 1.4 Hz), 7.7 (dd, Ar, 1H, J = 8.8, 1.1 Hz), and 7.8 (d, Ar, 1H, J = 1.2 Hz). FT-IR (KBr cm^{-1}): 2919 and 2850 (ν CH_2); 2231 (ν CN); 1613, 1527, and 1489 (ν C = C ring); 1269 (ν C–F); 1165 (ν C–O–C); 1025 (ν C–O); 882, 825 and 785 (δ C–H); and 666 (ν C–Br). FABHRMS: Observed (m/z) [M^+] 737.3624 (95.05%); Estimated (m/z) [M^+] 737.3619. *Anal* Calcd for $C_{43}H_{58}BrF_2NO_2$: C, 69.90; H, 7.91; Br, 10.81; F, 5.14; N, 1.90; O, 4.33. Found: C, 71.24; H, 8.59; N, 1.82.

2.2.4. 4-(ω-bromododecyloxy)-2′,3′,5′,6′-tetrafluoro-4″-dodecyloxy-1,1′:4′,1″terphenyl-3-carbonitrile (T4F-CN)

A procedure similar to that used for the synthesis of T2F-CN was followed. 1.06 g (2.17 mmol) of 5b, 0.1181 g (0.1 mmol) Pd[P(C_6H_5)$_3$]$_4$, 1 g (2.44 mmol) of 3-cyano-4-(ω-bromododecyloxy) phenylboronic acid, and 13.28 mL of Na_2CO_3 2 M (aqueous solution). The product was purified by using a silica gel chromatographic column and a hexanes:ethyl acetate (9:1) mixture. T4F-CN was obtained as a white solid (yield 81%). ^{1}H NMR ($CDCl_3$, δ = ppm) 0.8 (t, CH_3, 3H, J = 6.6 Hz), 1.2–1.6 (m, CH_2, 34 H), 1.7–1.9 (m, O-CH_2-CH_2, Br-CH_2-CH_2, 6 H), 3.4 (t, CH_2-Br, 2H, J = 6.9 Hz), 4.01 (t, O-CH_2-CH_2, 2H, J = 6.5 Hz), 4.12 (t, O-CH_2-CH_2, 2H, J = 6.5 Hz), 7.02 (d, Ar, 2H, J = 8.8 Hz), 7.09 (d, Ar, 1H, J = 8.8 Hz), 7.45 (d, Ar, 2H, J = 8.5 Hz), 7.66 (d, Ar, 1H, J = 8.8 Hz), and 7.73 (s, Ar, 1H,). FT-IR (KBr cm^{-1}): 2919 and 2851 (ν CH_2); 2232 (ν CN); 1612, 1525, and 1469 (ν C = C ring); 1256 (ν C–F); 1181 (ν C–O–C); 1027 (ν C–O); 822 and 724 (δ C–H); and 636 (ν C–Br). FABHRMS: Observed (m/z) [M^+] 773.3429 (20.93%); Estimated (m/z) [M^+] 773.3431. *Anal* Calcd for $C_{43}H_{56}BrF_4NO_2$: C, 66.66; H, 7.29; Br, 10.31; F, 9.81; N, 1.81; O, 4.13. Found: C, 67.09; H, 7.51; N, 1.83.

2.3. Instruments

The chemical structure of intermediates and final products was confirmed by proton and carbon nuclear magnetic resonance (^{1}H NMR and ^{13}C NMR) spectroscopy using a Jeol 300 MHz spectrometer and $CDCl_3$ or methanol-d_4 as solvent. The chemical structure was also studied by Fourier Transform Infrared (FTIR) spectroscopy (ATR method) using a 550 Nicolet Magna spectrophotometer. The elemental analysis was performed with a PerkinElmer 2400 Series II CHNS/O Elemental Analyzer. High resolution mass spectrometry was recorded on a Jeol JMS-700 MStation, Ion Mode: FAB$^+$ (Fast atom bombardment). The thermal stability of vacuum dried samples was determined with a thermogravimetric analyzer (TGA) from DuPont Instruments (TGA 951) connected to a N_2 vector gas, and heating at constant rate (10 °C min^{-1}) from 30 to 700 °C. The thermal behavior (phase transitions) was determined in a FP94HT differential scanning calorimeter (DSC) from Mettler at heating and cooling rates of 3 °C/min; reported traces correspond to the first cooling and second heating scans. The optical textures of mesophases were registered at different temperatures on cooling from the isotropic liquid, using a polarizing optical microscope (POM) from Olympus, coupled to a FP82HT heating plate from Mettler. The X-ray diffraction (XRD) analysis was performed in a SWAXS from Anton Paar (SAXSess mc^2) equipped with a sample holder unit (TCS 300-C), an image plate detector, and a temperature control unit (TCU50). X-rays (Cu k_α radiation; λ_{max} = 0.1542 nm) were generated at 40 kV and 50 mA. Each sample (finely powdered) was introduced into a glass capillary with outer diameter and wall thickness of 1.0 and 0.01 mm, respectively. XRD patterns were captured at different temperatures on cooling from the isotropic liquid. UV–vis spectra (190–820 nm) were recorded in a spectrophotometer from Shimadzu (UV-2401PC) using a standard quartz cell and spectrophotometric grade chloroform at a concentration of around 0.05 mg mL^{-1}. Finally, the fluorescence in solution (spectrophotometric grade $CHCl_3$ as solvent) was measured in a spectrofluorimeter from Perkin Elmer LS-50B. Procedures were identical for all samples.

3. Results and discussion

3.1. Synthesis

The semi-fluorinated *p*-terphenyls were synthesized through three reactions steps: *i*) alkylation of the 4-hydroxy-1-bromobenzene (with and without a cyano group) with a mono or dibromo-terminated dodecyl chain, *ii*) formation of the aryl boronic acids (2 and 4 in Scheme 1) using the alkylated bromobenzenes, BuLi and triisopropylborate, and *iii*) coupling of the alkylated phenyl boronic acids with a di or tetrafluorinated dibromobenzene via the Suzuki-Miyaura cross-coupling reaction using Pd[P(C_6H_5)$_3$]$_4$ as catalyst. [20] Here, only the step *iii* was detailed in the experimental section because the steps *i* and *ii* are similar to those described in a previous report. [19] As noted in the experimental part, T2F and T4F were obtained as byproducts in the synthesis of 5a and 5b, respectively. Despite the low yield (28% for T2F and 22.8% for T4F), the obtained amounts were enough for a full chemical, thermal and optical characterization.

The structure and purity of the four synthesized *p*-terphenyls were confirmed by ^{1}H NMR spectroscopy. Since all spectra are similar, only those corresponding to T2F-CN and T4F-CN were selected as examples (Fig. 1). It can be noted that, except for the typical singlet of $CDCl_3$ (7.26 ppm), all signals correspond to protons of the synthesized molecules (see inserts in Fig. 1). The only difference between the two spectra of Fig. 1 is the complex signal centered at 7.18 ppm in the spectrum of T2F-CN, and that corresponds to the d and e protons. Such complex signal is a double of doublets that indicates that protons d and e are coupled with the neighboring fluorine atoms. ^{13}C NMR and 2D NMR experiments (*Supplemental online information, S1-S6*) supported the accurate assignment.

3.2. Thermal behavior

The four synthesized *p*-terphenyls were first analyzed by TGA (*Supplemental online information, S7*) to determine their initial decomposition temperature, which was later considered as a limit temperature for their thermotropic analysis by DSC, POM and XRD. All four *p*-terphenyls resulted thermally stable up to 300 °C as is typical for *p*-terphenyl derivatives. [4] This temperature is far higher than the clearing temperature of any of them.

The DSC thermograms (Fig. 2) of two *p*-terphenyls showed multiple transitions associated to a mesomorphic behavior. One corresponds to T2F, which, upon cooling, developed four thermal transitions around 121, 119, 117 and 108 °C, and the other one corresponds to T2F-CN, which displayed two thermal transitions near 100 and 64 °C. As noted in the DSC traces, both T2F and T2F-CN are enantiotropic liquid crystals. T4F showed only one thermal transition around 131 °C, whereas T4F-CN displayed three broad thermal transitions corresponding to liquid-solid (108 °C), solid-solid (98 °C), and solid-solid (57 °C) transitions.

A non-fluorinated *p*-terphenyl (homologous to T2F and T4F) carrying one dodecyloxy chain at each one of the peripheral rings was synthesized and thermally characterized by us in a previous work [21]. Its DSC thermogram displayed four mesomorphic regions that were associated to different smectic phases as therein deduced from XRD results. The melting and clearing temperatures of such a non-fluorinated *p*-terphenyl are 130 and 205 °C, respectively. These transition temperatures are higher than the corresponding ones for T2F (113 and

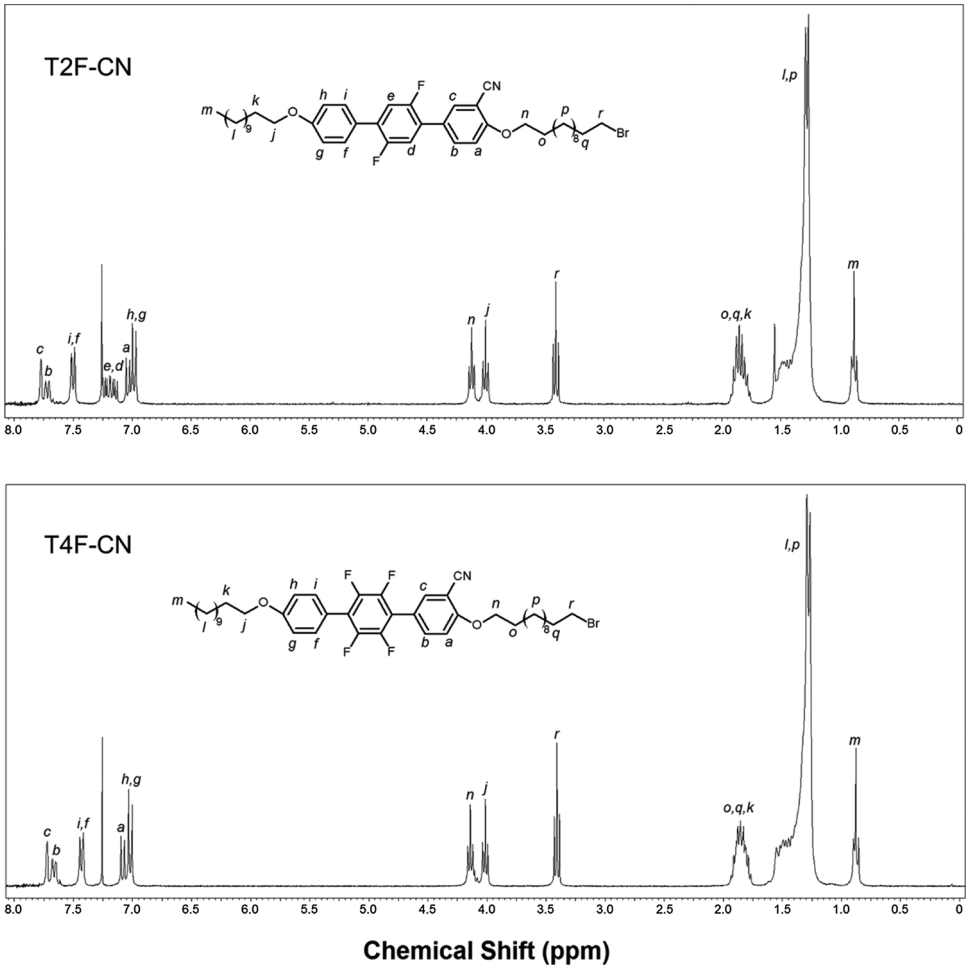

Fig. 1. ^{1}H NMR spectra of T2F-CN and T4F-CN ($CDCl_3$). In order to make comparison between spectra easier, protons were signaled with the same letters (note that letters *d* and *e* were omitted in the spectrum of T4F-CN).

122 °C, respectively), although the melting temperature (130 °C) is close to that shown by T4F (~134 °C). From this comparison it is clear that the substitution of two hydrogens for two fluorine atoms has produced a shifting of the mesomorphic behavior towards lower temperatures. The substitution of the all four hydrogens of the central ring (T4F) resulted in a *p*-terphenyl derivative showing no liquid crystalline properties.

The phase transitions detected by DSC were next corroborated by polarizing optical microscopy. Observations were made at different temperatures on cooling from the isotropic phase. At 121 °C, T2F showed droplets (Fig. 3A) that merged into a schlieren texture (Fig. 3B) typical of a nematic phase. Then, at 119 °C the schlieren texture changed into a focal conic fan texture (Fig. 3C) that almost instantly (at 118 °C) turned into a broken fan-shape texture (Fig. 3D). [22] The mesophase observed between 119 and 118 °C was not detected in further XRD studies, but according to the optical texture it can be attributed to a smectic-A phase. On the other hand, T2F-CN displayed at 99 °C a focal-conic fan texture (micrograph not shown here) that remain unchanged up to 65 °C where it crystallized.

In most works on the thermotropic behavior of fluorine-substituted *p*-terphenyl liquid crystals, nematic and/or low ordered smectic phases were reported. For instance, Choluj et al., studied the thermotropic behavior of series of *p*-terphenyls substituted with one, two or three fluorine atoms, and they found that the number of mesophases decreases as the number of fluorine atoms in the *p*-terphenyl core increases, in such a way that those *p*-terphenyls substituted with three fluorine atoms (in a variety of positions) develop only a nematic phase [9]. For *p*-terphenyls substituted with two fluorine atoms in the central ring (in *ortho* position the one to the other) they observed only one nematic phase, while for those having the two fluorine atoms in a peripheral ring they have encountered nematic and smectic A (or smectic C) phases. Goodby et al. have found similar results in *p*-terphenyls substituted with two fluorine atoms either in the central or in a peripheral ring [2]. Our T2F molecule (fluorine atoms in *para* position) showed these three mesophases with the smectic C phase over a larger temperature interval. T2F-CN developed only one mesophase, although in this compound the thermal behavior depends on the effects of both fluorine and cyano groups.

The nature and structure of the observed mesophases was assessed from the X-ray diffraction patterns recorded at different temperatures on cooling from the isotropic phase. At 120 °C, T2F displayed one broad peak at both low and wide angles of the X-ray pattern (Fig. 4), corroborating the presence of a non-ordered phase of the nematic type. On cooling to 116 °C, the diffuse peak at low angles turned into a sharp Bragg reflection (indexed as 001) while the broad peak remained unchanged. The sharp peak was attributed to the stacking period (d_{001}) of a smectic phase. d_{001} (41 Å) was then compared with the length of the molecule in its most extended conformation *L* (45.4 Å), calculated by molecular modelling software from Spartan (Spartan 10). Results showed that d_{001}/L is slightly smaller than unity, suggesting a single layer stacking with molecules tilted (25.4°) with respect to the normal of the smectic plane [23]. On the other hand, T2F-CN showed a sharp Bragg reflection (001) at low angles and a broad peak at wide angles, also indicating a smectic phase of low order. In comparing d_{001} (39.6 Å)

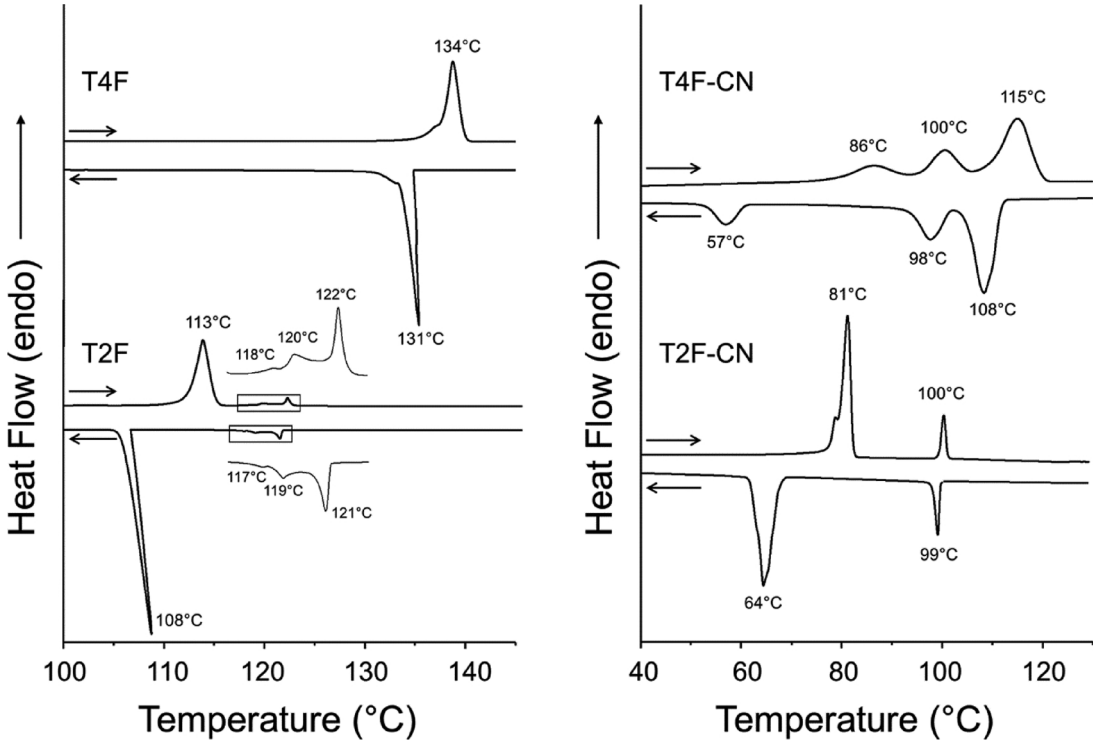

Fig. 2. DSC thermograms of the semi-fluorinated *p*-terphenyls.

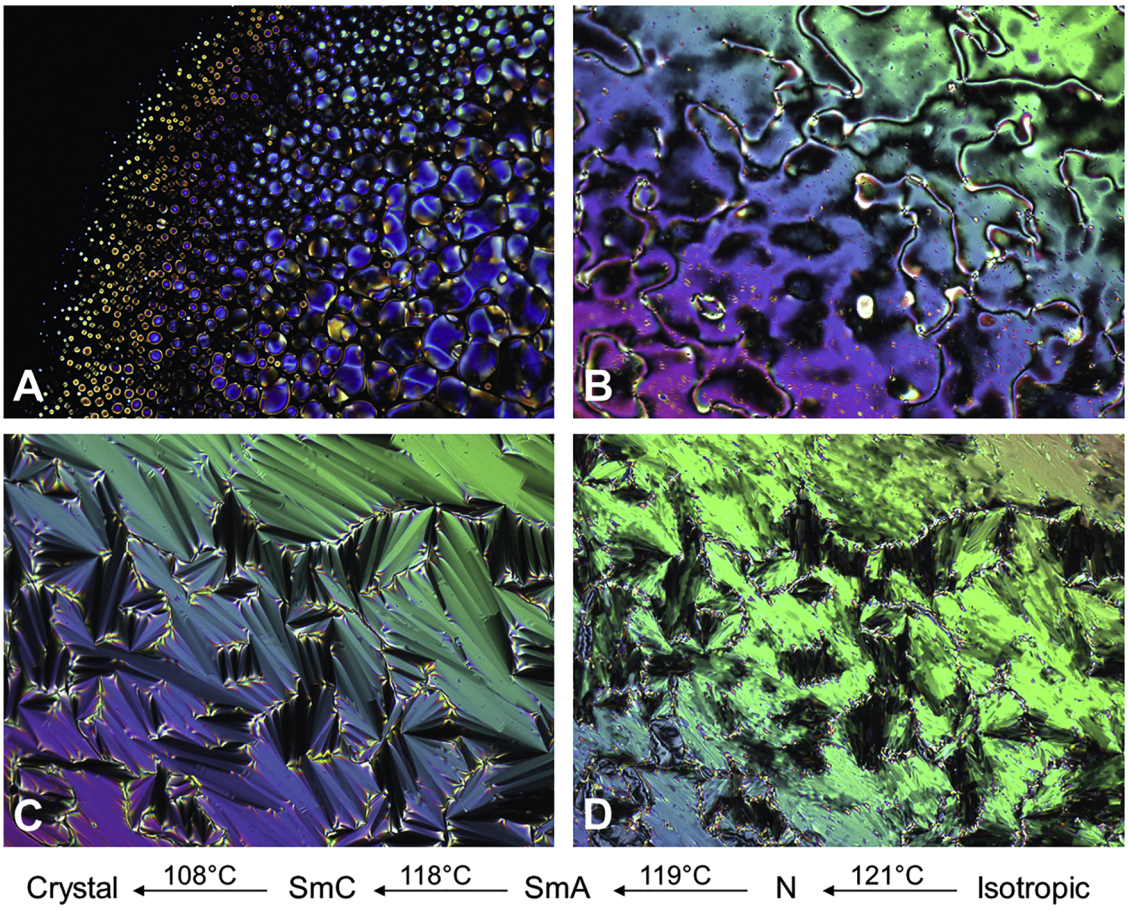

Fig. 3. Optical textures of T2F captured at different temperatures (T_A = 121 °C, T_B = 119 °C, T_C = 118.5 °C, and T_D = 116 °C) on cooling from the isotropic phase.

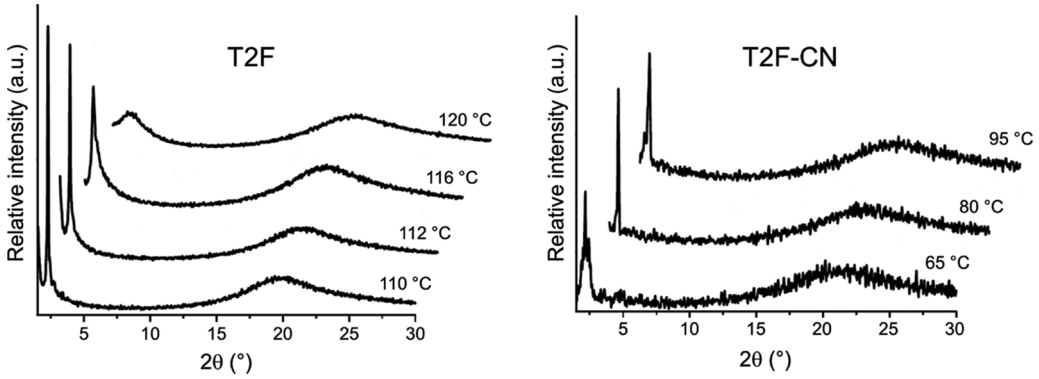

Fig. 4. X-ray diffraction analysis of *p*-terphenyls substituted with two fluorine atoms registered at various temperatures upon cooling from the isotropic liquid.

Table 1
Thermal properties and structural parameters for T2F and T2F-CN.

Molecule	*T* (°C)	d_{001} (Å)	*L* (Å)	*d/L*	Stacking	Tilt angle (°)	Thermal transitions [b] (°C)
T2F	116	41	45.4	0.9	Single layer	25.4 [a]	I 121 N 119 SmA 118 SmC 108 Cr
T2F-CN	80	39.6	46.0	0.86	Single layer	30.6	I 100 SmC 64 Cr

a)For the SmC phase. b)Upon cooling.

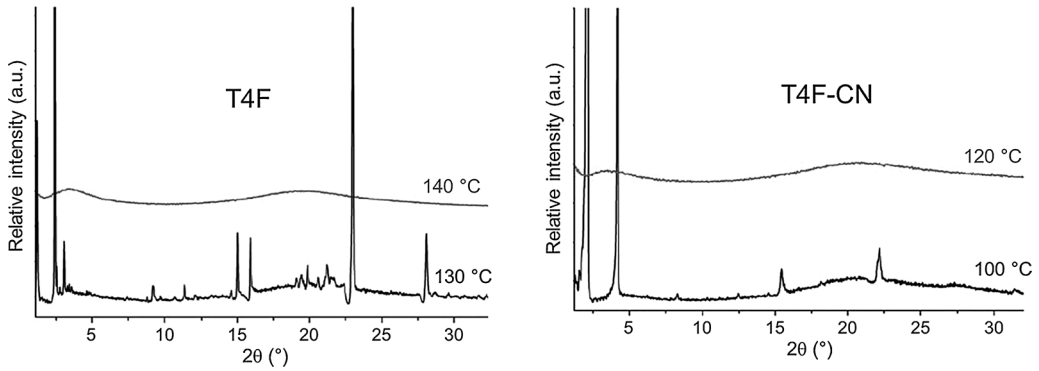

Fig. 5. X-ray diffraction patterns of *p*-terphenyls substituted with four fluorine atoms registered at two different temperatures.

with *L* (46.0 Å) a single-layered smectic C phase was also concluded for this derivative. The thermal transitions and the structural parameters for T2F and T2F-CN are gathered in Table 1. For T4F and T4F-CN the multiple peaks across the X-ray pattern confirmed their crystalline nature (Fig. 5).

Partially fluorinated *p*-terphenyl liquid crystals have intensely been studied from the stand point of thermal properties and structural characteristics [2,16]. In general, the fluorine atoms tend to depress the melting temperature, decrease the mesomorphic stability, and increase the probability of mesophases of low order like nematic, smectic A and smectic C phases [9,10]. A full exchange of hydrogens by fluorine atoms in the benzene ring inverses its electron density distribution [24]. In polyaromatic molecules having both perfluorinated (electron poor) and non-fluorinated (electron rich) rings, the $\pi - \pi_F$ interactions are supposed to prevail over the $\pi - \pi$ interactions [25]. The $\pi - \pi_F$ interactions may therefore stabilize the stacking of molecules in a specific configuration, depending on which rings (and how) are fluorinated [26]. For *p*-terphenyls carrying fluorine atoms in the central ring, zig-zag (Fig. 6B) and staggered (Fig. 6C) configurations are expected to occur since both configurations let the electron rich rings associate with the electron poor rings of neighboring molecules through $\pi - \pi_F$ interactions. The staggered packing has already been proposed by Goodby et al. for fluorine-substituted *p*-terphenyls [2]. Therein, it was suggested that the staggered arrangement induces the formation of tilted smectic phases, as was indeed found in the *p*-terphenyls studied the present work. According to the electron density distribution (Fig. 7), the $\pi - \pi_F$ interaction must be stronger in the stacks of T4F than in those of T2F. The measured higher melting temperature of T4F is possibly due to a close packing of molecules arising from such stronger $\pi - \pi_F$ interaction. For T2F, the electron density distribution lets the molecules stack through $\pi - \pi_F$ interactions but much weaker. Its low melting temperature, as well as its ability to develop liquid crystals phases, are likely associated to these weaker interactions. The presence of a cyano group in *p*-terphenyls (T2F-CN and T4F-CN) also affects the way they arrange by themselves in a mesophase or in a crystalline structure. The relatively high bulkiness of this group (as compared to hydrogen and fluorine atoms) hinders the close packing of molecules, although, its high electron withdrawing character produces other type of interactions, like the C–H… N interaction that is relatively weak but that can determine the crystal packing of molecules carrying both fluorine atoms and cyano groups. This is the case of some fluorobenzonitriles whose crystal packing is directed by the C–H…N interaction [27]. In our T2F-CN and T4F-CN molecules, the C–H…N interaction can contribute to determining both the molecular packing and the thermal properties. Compared to T2F, T2F-CN showed lower melting and clearing temperatures, suggesting that the cyano group perturbs the interaction between *p*-terphenyls but to a limited extent since it is still able to develop liquid crystal properties. T4F-CN showed a lower melting temperature than T4F, but even so, it is not able to develop a liquid crystal behavior.

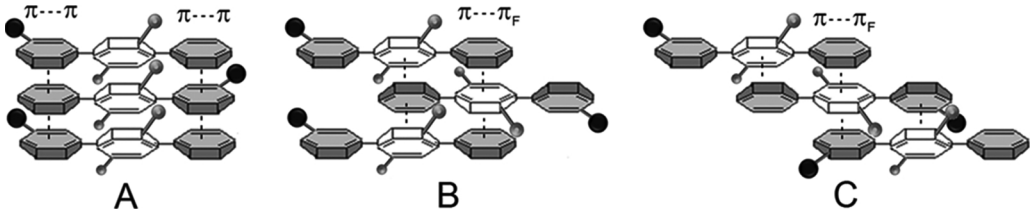

Fig. 6. Stacking of T2F-CN in the smectic phase. The zig-zag (B) and staggered (C) configurations are stabilized by π – π_F interactions. Configuration A is not favorable from the interactional point of view. The alkoxy chains were omitted.

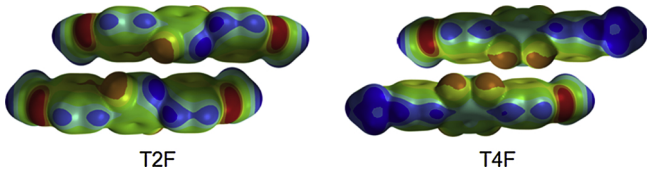

Fig. 7. Electron density distribution of T2F and T4F stabilized through π – π_F interactions. Modeled molecules have two methoxy groups (one at each end of the *p*-terphenyl) instead of two dodecyloxy chains.

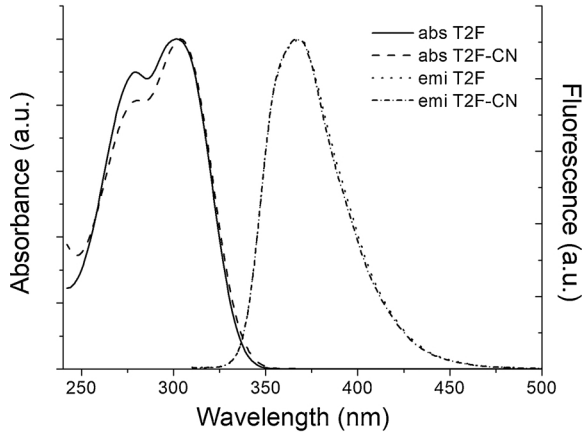

Fig. 8. UV–vis absorption and emission spectra of *p*-terphenyls substituted with two fluorine atom and with (T2F-CN) or without (T2F) cyano group. $CHCl_3$ was used as solvent.

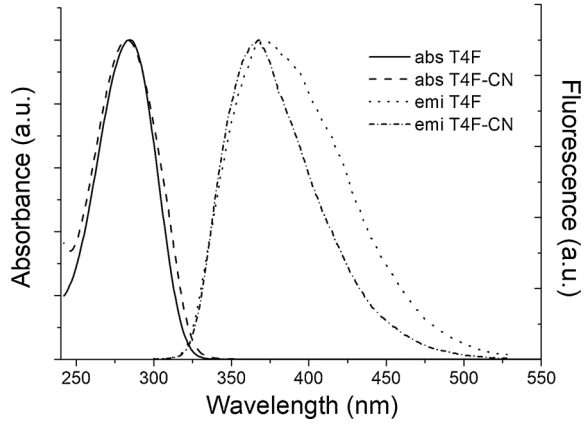

Fig. 9. UV–vis absorption and emission spectra of *p*-terphenyls substituted with four fluorine atoms, and with (T4F-CN) or without (T4F) cyano group. $CHCl_3$ was used as solvent.

3.3. Optical properties

Besides their ability to develop liquid crystal properties, *p*-terphenyls are known for their optical and photo-physical properties that have resulted potentially useful for applications as light emitting materials [28], wavelength shifters [29], scintillators [30], among others [31]. Their relatively large band gap energy (~ 3.5 eV) makes them blue-emitting materials [32]. The introduction of high electron-withdrawing substituents, like fluorine and cyano groups, lowers the HOMO/LUMO levels and therefore facilitates or allows the tuning of some electro-optical processes, like the electron injection in OLEDs [33].

The UV–vis absorption and emission spectra of the semi-fluorinated *p*-terphenyls were obtained in solution, using spectrophotometric grade chloroform as solvent. The absorption spectra of T2F and T2F-CN displayed two partially superposed bands with maxima (λ_{max}) around 280 and 303 nm (Fig. 8), whereas those of T4F and T4F-CN showed one single band with λ_{max} around 284 nm (Fig. 9). As known, the shape, intensity, and position of the absorption bands of π-conjugated molecules depend on the conjugation length, conformation (planarity), nature and number of substituents, among others [3,16,34]. In solution, the band position also depends on the solvent polarity [35]. For the *p*-terphenyl without fluorine atoms (control) the measured λ_{max} in chloroform is 268 nm [3], therefore, the substitution of two or four hydrogens for fluorine atoms has produced a bathochromic effect (red shift). T4F and T4F-CN absorb at lower wavelength (λ_{max} = 284 nm) as compared to T2F and T2F-CN (λ_{max} = 303 nm) due to steric effects that make the tetrafluoro-substituted *p*-terphenyls more twisted than the difluoro-substituted ones, perturbing in larger extent the conjugation of π-orbitals (associated to the planarity). A similar effect was observed by Seed et al. in studying *ortho* and *meta* monofluoro-substituted biphenyls [34]. These authors found that the *meta*-substituted biphenyls absorb at higher wavelength (lower energy) than the *ortho*-substituted ones due to their lower interannular torsion angle that makes the π-conjugation more effective. The two absorption bands in the spectra of T2F and T2F-CN were attributed to transitions between localized orbitals (lower wavelengths) and conjugation of phenyl rings (high wavelengths) [3]. The molar absorptivity (ε) of each semi-fluorinated *p*-terphenyl was graphically determined (Fig. 10), and resulting values are gathered in Table 2. It can be readily noticed that ε increases markedly from the two to the four fluorine-substituted *p*-terphenyls, meaning that the introduction of more fluorine atoms makes the *p*-terphenyl core a stronger absorbing specie. As noted, neither the shape nor the position of absorption bands was affected by the cyano group. A similar result was observed in a previous study on the UV–vis absorption characteristics of *p*-terphenyls (non-fluorinated) laterally substituted with zero, one or two cyano groups [32]. The optical band gap (Eg_{opt}) and the fluorescence quantum yield (Φ) were measured in solution ($CHCl_3$ as solvent) for the four semi-fluorinated terphenyls (Table 2). Eg_{opt} values of 3.54 and 3.8 eV indicate that all four compounds are semiconducting materials. The quantum yield (between 44 and 60%) is relatively high and comparable to that reported for other terphenyls [32,36].

All four fluorinated compounds were next excited with a monochromatic UV light 10 nm below λ_{max}. The recorded spectra showed that all four chromophores fluoresce at almost the same wavelength interval with maximum around 367 nm (Figs. 8 and 9). Only T4F showed a slightly red-shifted (λ_{max} = 372) and broader (HHBW = 90 nm) emission band, suggesting that for this compound more conformers in the excited state are emitting. The large Stokes shift ($\triangle\nu$ ~ 8200 cm^{-1}), associated to a change from a high energy twisted conformer in the ground state to a lower energy planar (quinoid) conformer in the excited state, makes these materials nearly transparent to their own emitted light [32,35]. These preliminary results may be

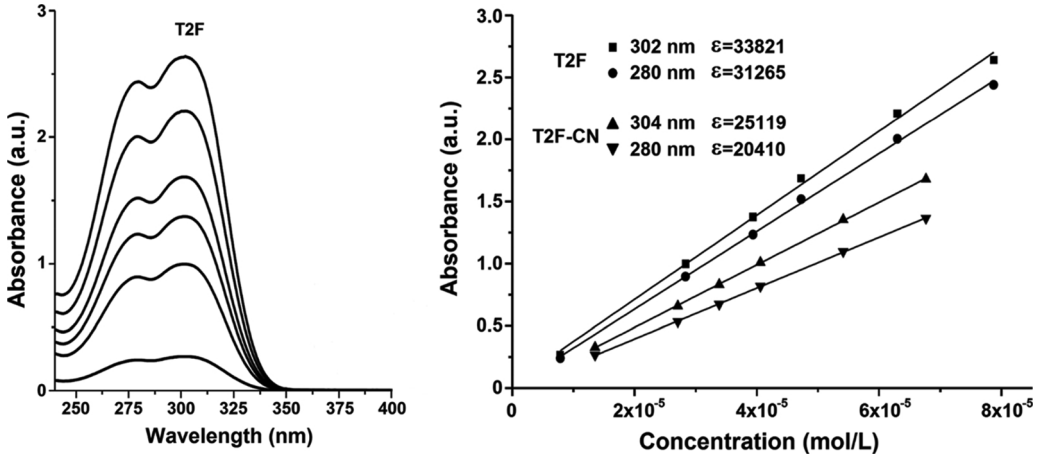

Fig. 10. UV–vis absorption spectra of T2F at different concentrations (left), and absorbance (measured at two λ_{max}) versus concentration plots for T2F and T2F-CN (right). $CHCl_3$ was used as solvent.

Table 2
UV–vis absorption and emission properties of the semi-fluorinated *p*-terphenyls in solution (chloroform as solvent).

	$\lambda_{max\ abs}$ (nm)	$HHBW_{abs}$ (nm)	$\lambda_{max\ emi}$ (nm)	$HHBW_{emi}$ (nm)	$\triangle\upsilon$ (cm^{-1})	ε ($M^{-1}\,cm^{-1}$)	Eg_{opt} (eV)	Φ (%)
T2F	280	66	367	47	5,864	33,821	3.54	52
	302					31,265		
T4F	285	45	372	90	8,206	38,249	3.80	60
T2F-CN	280	66	367	47	5,646	25,119	3.54	56
	304					20,410		
T4F-CN	283	51	368	65	8,161	40,595	3.80	44

complemented with further work on photo-physical properties to evaluate the potential application as for instance in linearly polarized organic light-emitting diodes (OLEDs) profiting of the liquid-crystalline properties and the high energy emission (blue region) shown by these semi-fluorinated *p*-terphenyls.

4. Conclusion

Four *p*-terphenyls laterally substituted with fluorine and cyano groups were synthesized and their thermotropic properties were characterized by DSC, POM and XRD. Their light absorption and emission (fluorescence) were also characterized. Only two of the four compounds developed liquid crystal properties. One of them showed a N – SmA – SmC sequence while the other showed only a SmC phase. This smectic phase was determined to be single layer type with a staggered configuration stabilized by $\pi - \pi_F$ interactions. On the other hand, the UV–vis optical characterization showed that all four compounds absorb and fluoresce in the blue region of the electromagnetic spectrum. The measured large Stokes shift indicates that the semi-fluorinated *p*-terphenyls are nearly transparent to their own emitted light. Finally, in this research work we have synthesized new fluorinated *p*-terphenyls combining low ordered (or low viscous) liquid crystal phases with a high energy light emission (blue light), a combination that is potentially useful for developing linearly polarized electro-optical devices.

Acknowledgements

The authors wish to thank the Consejo Nacional de Ciencia y Tecnología (CONACYT) of Mexico for the financial support of this work (Project CB 242232). MVP also thanks CONACYT for the grant given during his Master in Sciences studies.

Appendix A. Supplementary data

Supplementary material related to this article can be found, in the online version, at doi:https://doi.org/10.1016/j.jfluchem.2018.11.011.

References

[1] Z.N. Yu, H.L. Tu, X.H. Wan, X.F. Chen, Q.F. Zhou, Mol. Cryst. Liq. Cryst 391 (2003) 41.
[2] J.W. Goodby, I.M. Saez, S.J. Cowling, J.S. Gasowska, R.A. MacDonald, S. Sia, P. Watson, K.J. Toyne, M. Hird, R.A. Lewis, S.E. Lee, V. Vaschenko, Liq. Cryst. 36 (2009) 567.
[3] L. Larios-López, D. Navarro-Rodríguez, E.M. Arias-Marín, I. Moggio, C.V. Reyes-Castañeda, Liq. Cryst. 30 (2003) 423.
[4] W. Ried, D. Freitag, Angew. Chem. Int. Ed. 7 (1968) 835.
[5] J.S. Gasowska, S.J. Cowling, M.C.R. Cockett, M. Hird, R.A. Lewis, E.P. Raynes, J.W. Goodby, J. Mater. Chem. 20 (2010) 299.
[6] P. Kula, A. Spadlo, J. Dziaduszek, M. Filipowicz, R. Dabrowski, J. Czub, S. Urban, Opto-electron, Rev. 16 (2008) 379.
[7] A. Parish, S. Gauza, S.T. Wu, J. Dziaduszek, R. Dabrowski, Mol. Cryst. Liq. Cryst. 489 (2008) 348.
[8] M. Hird, Chem. Soc. Rev. 36 (2007) 2070.
[9] A. Choluj, P. Kula, R. Dabrowski, M. Tykarska, L. Jaroszewicz, Mater. Chem. C 2 (2014) 891.
[10] S. Matharu, S.J. Cowling, G. Wright, Liq. Cryst. 34 (2007) 489.
[11] T.H. Lee, C.S. Hsu, Liq. Cryst. 41 (2014) 1235.
[12] P. Kula, J. Herman, S. Pluczyk, P. Harmata, G. Mangelinckx, J. Beeckman, Liq. Cryst. 41 (2014) 503.
[13] M.J. Goulding, Greenfield S, D. Coates, R. Clemitson, Liq. Cryst. 14 (1993) 1397.
[14] A.A. Kiryanov, P.Sampson.A.J. Seed, J. Mater. Chem. 11 (2001) 3068.
[15] G.W. Gray, K.J. Harrison, J.A. Nash, J.C.S. Chem. Comm. (1974) 431.
[16] R. Dabrowski, P. Kula, J. Herman, Crystals 3 (2013) 443.
[17] L. Oriol, M. Piñol, J.L. Serrano, C. Martínez, R. Alcalá, R. Cases, C. Sánchez, Polymer 42 (2001) 2737.
[18] F. Peng, H. Chen, S. Tripathi, R.J. Twieg, S.T. Wu, Opt. Mater. Express 5 (2015) 265.
[19] T. García, L. Larios-López, R.J. Rodríguez-González, G. Martínez-Ponce, C. Solano, D. Navarro-Rodríguez, Polymer 53 (2012) 2049.
[20] N. Miyaura, A. Suzuki, Chem. Rev. 95 (1995) 2457.
[21] M.L. Mota-González, A. Carrillo-Castillo, R.C. Ambrosio-Lázaro, J. Flores Méndez, M. Moreno, P.A. Luque, D. Navarro, J. Chem. (2017) ID 8275489.
[22] I. Dierking, Textures of Liquid Crystals, Wiley-VCH, Weinheim, 2003.
[23] R.G. Santos Martell, A. Ceniceros-Olguin, L. Larios-López, R.J. Rodríguez-González,

D. Navarro-Rodríguez, B. Donnio, D. Guillon, Liq. Cryst. 36 (2009) 787.
[24] J. Vrbancich, G.L.D. Ritchie, J.C.S. Faraday II, 76 (1980) 648.
[25] R. Berger, G. Resnati, P. Metrangolo, E. Weber, J. Hulliger, Chem. Soc. Rev. 40 (2011) 3496.
[26] Y. Sonoda, M. Goto, S. Tsuzuki, H. Akiyama, N. Tamaoki, J. Fluor. Chem. 130 (2009) 151.
[27] V. Vasylyeva, K. Merz, Cryst. Growth Des. 10 (2010) 4250.
[28] H.R. Liao, Y.J. Lin, Y.M. Chou, F.T. Luo, B.C. Wang, J. Lumin. 128 (2008) 1373–1378.
[29] S. Joosten, E. Kaczanowicz, M. Ungaro, M. Rehfuss, K. Johnston, Z.E. Meziani, Nucl. Inst. Methods in Phys Res A 870 (2017) 110.
[30] O.V. Dudnik, L.A. Andryushenko, V.A. Tarasov, E.V. Kurbatov, Instrum. Exper. Tech. 58 (2015) 206.
[31] D.J. Schneider, D.A. Landis, P.A. Fleitz, C.J. Seliskar, J.M. Kauffman, R.N. Stepel, Laser Chem. 11 (1991) 49.
[32] I. Felix-Serrano, N. Trejo-Carbajal, R.J. Rodríguez-González, L. Larios-López, I. Moggio, E. Arias, J.R. Torres-Lubián, D. Navarro-Rodríguez, J. Mol. Liq. 241 (2017) 347.
[33] F. Babudri, G.M. Farinola, F. Naso, R. Ragni, Chem Comm. (2007) 1003.
[34] A.J. Seed, K.J. Toyne, J.W. Goodby, J. Mater. Chem. 5 (1995) 2201.
[35] K.L. Liu, Y.T. Chen, H.H. Lin, C.S. Hsu, H.W. Chang, I.C. Chen, J. Phys. Chem. C 115 (2011) 22578.
[36] L. Li, M. Chen, H. Zhang, H. Nie, J.Z. Sun, A. Qin, B.Z. Tang, Chem. Comm. 51 (2015) 4830.